Geothermics 53 (2014) 236–254

Contents lists available at ScienceDirect

Geothermics

journal homepage: www.elsevier.com/locate/geothermics

Invited Review

Geothermal steam-water separators: Design overview

Sadiq J. Zarrouk[a,*], Munggang H. Purnanto[b]

[a] Department of Engineering Science, The University of Auckland, New Zealand
[b] Facilities Department, Star Energy Geothermal (Wayang Windu) Ltd., Indonesia

ARTICLE INFO

Article history:
Received 26 February 2014
Accepted 29 May 2014

Keywords:
Geothermal separator
Cyclone
Separator efficiency
Vertical separator
Horizontal separator
CFD modelling

ABSTRACT

Since the development of the liquid dominated geothermal reservoir at Wairakei, New Zealand in 1950s, various separator designs have been utilised to enable the separation of steam and water from two-phase geothermal fluid. This is to ensure that only dry and clean steam enters the turbine and generates electricity. Information from several existing geothermal fields shows that there are two common separator designs, the vertical cyclone separator and the horizontal separator. Both designs are reported to have high separation efficiency in the order of 99.9% or higher. The vertical cyclone separator is normally found at power stations with strong influence by the technology from New Zealand. The horizontal separator is normally found at power stations with strong influence by technology from Iceland, Japan, Russia and the US.

The vertical cyclone designs are based on the experience in Wairakei and Kawerau in the 1950s and 1960s, and the modelling work by Lazalde-Crabtree's (1984). While the principles of the geothermal horizontal separator design were only reported by Gerunda (1981).

This paper reviews the steam-water separator designs that are commonly used in geothermal steam fields worldwide. The general steps to design the separator for any given geothermal fluid are presented. This is starting from the selection of optimum separation pressure, predicting the separator efficiency and calculating the internal pressure drop.

Recent research that utilises the numerical approach using Computational Fluid Dynamics (CFD) to obtain better understanding of the fluid behaviour within the separator is reported.

Unpublished data from the early 1950s Wairakei trials are presented in this work. They show that the breakdown velocity increases with the reduction in the internal diameter of separator body. The measurement of the separator efficiency is also discussed.

Practical design aspects for the optimum locating of the separator and the main separator design considerations are also given. Recent concepts in separator designs are also presented and discussed.

Contents

* Corresponding author at: Department of Engineering Science, The University of Auckland, Private Bag 92019, Auckland, New Zealand. Tel.: +64 9 373 7599x85542; fax: +64 9 373 7468.
E-mail addresses: s.zarrouk@auckland.ac.nz, sadiqzarrouk@gmail.com (S.J. Zarrouk).

http://dx.doi.org/10.1016/j.geothermics.2014.05.009
0375-6505/

Nomenclature

A	surface area (m^2)
A_o	surface area of inlet pipe (m^2)
A_e	inlet width (m)
B_e	inlet height (m)
C_{sb}^{Na}	concentration of sodium in separated brine (mg/kg)
$\dot{C}_S^{Na}$	mass flow rate of sodium in the separated steam (mg/s)
D	diameter (m)
D_t	inlet pipe diameter (m)
D_e	steam outlet pipe diameter (m)
D_b	water outlet pipe diameter (m)
d_w	drop diameter (m)
f_{av}	fractional area
f_{hv}	fractional height
h	enthalpy (kJ/kg)
j	dimensionless parameter given by Eq. (26)
K'	A coefficient for Eq. (3) (m/s)
K_c	dimensionless parameter given by Eq. (17)
L	length (m)
$\dot{m}$	mass flow rate (kg/s)
$\dot{m}_s$	mass flow rate of steam (kg/s)
$\dot{m}_f$	mass flow rate of fluid (kg/s)
$\dot{m}_w$	mass flow rate of water (kg/s)
$\dot{m}_b$	mass flow rate of brine carryover (kg/s)
$\dot{m}_L$	mass flow rate of liquid (kg/s)
$\dot{m}_G$	mass flow rate of gas (kg/s)
$\dot{m}_{VL}$	mass velocity of the liquid (kg/m^2 s)
$\dot{m}_{VG}$	mass velocity of the gas (kg/m^2 s)
n	free vortex coefficient (dimensionless)
NH	dimensionless parameter given by Eq. (29)
P	pressure (Pa, unless specified differently)
Q_{VS}	volumetric steam flow (m^3/s)
Q_L	volumetric water flow (m^3/s)
Re	Reynolds number (ratio of fluid's inertial force to its viscous forces, dimensionless)
Sp	separated water purity
T	temperature (°C, unless specified differently)
TDS	Total Dissolved Solids in the brine (ppm)
t_r	residence time (s)
t_{ma}	maximum additional time of steam in cyclone (s)
t_{mi}	average minimum residence time of steam in cyclone (s)
u	tangential inlet velocity (m/s)
v_t	terminal velocity (m/s)
v_h	velocity in the horizontal direction (m/s)
V	volumetric flow rate (m^3/s)
V_{AN}	upward annular steam velocity (m/s)
V_{OS}	volume defined in Fig. 11 (m^3)
V_{OH}	volume defined in Fig. 11 (m^3)
We	Weber number (ratio of fluid's inertia and its surface tension, dimensionless)
X_i	steam dryness (dimensionless)
ρ_L	density of liquid (kg/m^3)
ρ_G	density of gas (kg/m^3)
ρ_v	density of vapor (kg/m^3)
ρ_{air}	density of air (kg/m^3)
ρ_{water}	density of water (kg/m^3)
σ	surface tension (N/m)
σ_{water}	surface tension water (N/m)
ψ'	centrifugal inertia impaction parameter
η	efficiency (%)
η_{eff}	effective efficiency (%)
η_s	actual efficiency (%)
η_m	centrifugal efficiency (%)
η_A	entrainment efficiency (%)
μ_L	dynamic viscosity of water (poise)
μ_v	dynamic viscosity of vapour (kg/m s)

1. Introduction

The energy from geothermal fluid can be converted into electricity by utilising the geothermal steam as the working fluid to rotate the turbine which is coupled with the generator. Since turbine design usually requires a high steam quality at the inlet, i.e. the geothermal steam should be as dry as possible or slightly superheated. A small quantity of water carried over can cause major problems due to the fact that geothermal water contains dissolved minerals (solids) that may form scale deposition on the turbine blades, casing and nozzles reducing the turbine's conversion efficiency (Zarrouk and Moon, 2014). Water entrainment in the inlet steam on the other hand can cause erosion damage to the turbine rotor, blades and nozzles (communications with Mr. Chris Morris, Contact Energy Ltd.).

In dry geothermal fields, separators are not required. However, dry steam reservoirs are rare and only found in few fields around the world: Lardarello (Italy), the Geysers (USA), as well as limited dry steam areas in Matsukawa (Japan), Darajat and Kamojang (Indonesia), and Cove Fort Utah (USA) (Di Pippo, 2012). Most of the remaining conventional geothermal fields worldwide are liquid-dominated reservoirs producing a mixture of steam and water therefore separators are required (Zarrouk and Moon, 2014).

Challenges to develop wet fields for power generation had resulted in the development of steam-water separators. The separator enables the separation of steam and water from two-phase geothermal mixtures so that only steam is sent to run the turbine. Wairakei geothermal power station, New Zealand, was the first

Fig. 1. The U-bend separator installed together with TOC separator as seen in the Wairakei Field (picture by Sadiq Zarrouk, 1997).

plant to use a separator in the 1950s. Its successful design was then adopted by many fields around the world with very little change up to present (Foong, 2005).

2. The geothermal separator

The earliest method to separate steam and water is by passing the mixture into a large drum, called a knock out drum. Flashing occurs due to the drop in the fluid pressure and the less dense steam will rise up while the more dense water will fall down to the bottom of the drum (Foong, 2005).

Another method to remove water from the mixture is by using 180° U-bend separator which works through centrifugal effects. This separator is simple in design and is able to remove up to 80% of water. To further increase its dryness, the U-bend separator was installed in series with cyclone separator (Fig. 1). However, later designs quickly excluded the U-bend separator since the cyclone itself is capable of removing almost all of the water.

Currently, the cyclone separator is the most popular design found in most geothermal power stations around the world. Separation process is carried out by generating centrifugal force on the mixture entering the separator by using a tangential or spiral inlet to the cyclone. As the fluid rotates, the liquid with higher density will move outward and downwards while the vapour which has lower density will move inward and upward.

The cyclone separator has undergone several improvements to maximise its efficiency. In early designs, the steam was discharged at the top of the vessel while the brine was discharged from the bottom of the vessel (Fig. 2). This separator was referred to as top outlet cyclone separator (TOC) also known as the Woods separator. It was designed by Merz and McLellan and is used in some geothermal bores at Wairakei. The performance can be improved by up to 20% if installed (in series) together with U-bend separator (Bangma, 1961).

Having improved its efficiency, the top outlet cyclone separator was then superseded by the bottom outlet cyclone separator (BOC) also known as the Weber separator. In this design, the steam pipe is placed inside the vessel and leaves from the bottom of the separator. The BOC is popular because of its simplicity and also because separated steam is removed at the bottom of the separator instead of the top. This causes the steam line to support itself on a pipe near ground level, making it much simpler than the TOC (Bangma, 1961).

Despite the popularity of the vertical cyclone separator, Povarov et al. (2003) and Povarov and Nikolskiy (2003, 2005) argued that the new design of horizontal separator developed/used in the Mutnovsky Power Station, Russia has better efficiency and mass-dimension characteristics. The design is based on the experience

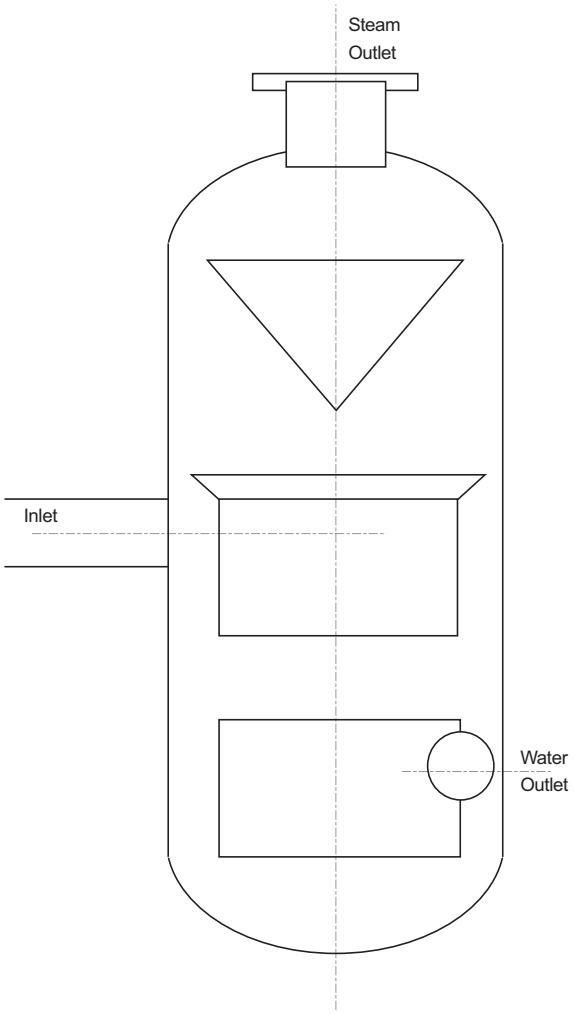

Fig. 2. The top outlet cyclone (TOC) separator (after Bangma, 1961).

of designing steam generators in nuclear power stations using the same mechanism for gravitational separation of liquid particles.

During 1967–1995, all separators constructed and installed in Iceland were of the vertical type. The horizontal type fitted with droplet elimination mats began to gain popularity in later years (Eliasson, 2001). However, there is no published analysis for this design. Hence, direct comparison with the vertical design is not currently possible. The only available practical procedure for horizontal type design was reported by Gerunda (1981) on a liquid–vapour separator. Although some improvements might have made the recent designs slightly different from Gerunda's (1981), the principle of his design is the same as in geothermal separators.

3. Geothermal separators around the world

The vertical cyclone separator has gained popularity due to its simple design, absence of moving parts, low cost, low pressure drop and high output quality and efficiency (Hoffmann and Stein, 2007; Lazalde-Crabtree, 1984). Published data from several geothermal power stations around the world (Table 1) indicates that vertical cyclone separator dominates the design worldwide (Fig. 3).

The horizontal separator is used mostly by power plants that inherit the Icelandic technology or was modified from the Russian

Table 1
Geothermal separators used around the world.

Country	Field	Unit	Year	Type	MW rated	Sep. type	Notes	Ref.
Costa Rica	Miravalle	Wellhead Unit 1	1995	1-Flash backpressure	1 × 5	V.	Wellhead unit 1 and wellhead unit 3 have been dismantled in 1998.	Moya and Nietzen (2005) and Di Pippo (2008)
		Wellhead Unit 2	1996	1-Flash	1 × 5	N.A.	There are 7 separation stations that supply the steam needed for Wellhead Unit 1, Unit 1, Unit 2 and Unit 3.	
		Wellhead Unit 3	1997	1-Flash	1 × 5	N.A.		
		1	1994	1-Flash	1 × 55	V.	Binary plant uses waste brine from Unit 1, 2 and 3	
		2	1998	1-Flash	1 × 55	V.		
		3	2000	1-Flash	1 × 29	V.		
		5	2004	Binary	2 × 9.5	V.		
El Salvador	Ahuachapan	1	1975–1976	1-Flash	1 × 30	V.	The horizontal separator in Unit 3 is a flasher that is installed to recover low pressure steam from wasted hot water in Unit 1 and 2	Di Pippo (1980), Kozaki (1982) and Monterrosa and Lopez (2010)
		2	1975–1976	1-Flash	1 × 30	V.		
		3	1980	2-Flash	1 × 35	H.		
El Salvador	Berlin	Wellhead	1992	1-Flash	2 × 5	V.	Wellhead units have been retired	Horie (2001), Di Pippo (2008), Argueta (2011) and Fuji (2011)
		1	1999	1-Flash	1 × 28	V.		
		2	1999	1-Flash	1 × 28	V.		
		3	2006	1-Flash	1 × 40	N.A.		
		4	2007	Binary	1 × 9.2	N.A.		
Indonesia	Wayang Windu	1	2000	1-Flash	1 × 110	V.	There are 3 separators for each unit, sized at 40 MW each	Murakami et al. (2000) and Syah et al. (2010)
		2	2009	1-Flash	1 × 117	V.		
Indonesia	Gunung Salak	1	1994	1-Flash	1 × 55	V.	Gunung Salak is also known as Awibengkok	Soeparjadi et al. (1998), Di Pippo (2008) and Adiprana et al. (2010)
		2	1994	1-Flash	1 × 55	V.		
		3	1997	1-Flash	1 × 55	V.		
		4	1997	1-Flash	1 × 55	V.		
		5	1997	1-Flash	1 × 55	V.		
		6	1997	1-Flash	1 × 55	V.		
Mexico	Cerro Prieto I	1 and 2	1973	1-Flash	2 × 37.5	V.	The gathering system consists of cyclone separators at each well, with steam line to power station and brine line to evaporation pond	Di Pippo (2008)
		3 and 4	1979	1-Flash	2 × 37.5	V.		
		5	1981	2-Flash	1 × 30	V.		
	Cerro Prieto II	1 and 2	1984	2-Flash	2 × 110	V.	The gathering system consists of one pair of wellhead separator and flasher from each well	Di Pippo (2008)
	Cerro Prieto III	1 and 2	1985	2-Flash	2 × 110	V.		
	Cerro Prieto IV	1–4	2000	1-Flash	4 × 25	V.		Di Pippo (2008)
New Zealand	Mokai	1	1999	Flash-Binary	1 × 25, 6 × 5	V.	The hot brine from the separator is passed to the evaporator section of the hot water binary plant. The dry steam is passed into the backpressure steam turbine and delivered to the evaporator section of the binary cycle plant. Mokai 1 has 2 separators while Mokai 2 has only 1 separator	Di Pippo (2008)
		2	2005	Flash-Binary	1 × 34, 1 × 8	V.		
New Zealand	Rotokawa	Combined Cycle	1997	Flash-Binary	1 × 13, 3 × 4.5	V.	The dry steam from the separator is sent to the backpressure turbine. The hot brine from the separator is used for the binary plant. The exhaust steam from the turbine is also used for the binary plant	Legmann (1999), Legmann and Sullivan (2003) and Di Pippo (2008)
		Extension	2003	Binary	1 × 4.5	N.A.		Di Pippo (2008)
		Nga Awa Purua	2010	3-Flash	1 × 139	V.	Inlet steam pressure: HP = 23.5 bara; IP = 8.4 bara; LP = 2.3 bara	Horie (2009)
New Zealand	Kawerau	1	2008	2-Flash	1 × 95	V.	Inlet steam pressure: HP=11.3 bara; LP=1.8 bara	Horie (2009)

Table 1 (*Continued*)

Country	Field	Unit	Year	Type	MW rated	Sep. type	Notes	Ref.
New Zealand	Wairakei	The A station, the B station, binary plant	1958–1963	1 Flash, 3-Flash, Binary	Total = 193	V.	The A station consist of several small units rated at 6.5 MW and 11.5 MW. There are HP turbines (12.4 bar), IP turbines (3.45 bar) and LP turbines (0.345 bar). The B station consists of three units, each rated at 30 MW. The turbine was design to take IP steam from the A station	Thain and Carey (2009)
New Zealand	Ohaaki	1	1989	1-Flash	1 × 104	V.	Operating capacity is 70 MW	From author's experience
New Zealand	Te Huka	1	2010	Binary	1 × 23	V.	Also known as Tauhara 1	From author's experience
Iceland	Nesjavellir	1 and 2	1998	1-Flash	2 × 30	H.	The separation system consists of steam separators and mist eliminators. The brine and exhaust steam from the turbine are both used to heat the water for domestic use in Reykjavic	Eliasson (2001) and Di Pippo (2012)
		3	2001	1-Flash	1 × 30	H.		
		4	2005	1-Flash	1 × 30	H.		
Iceland	Hellisheidi	1 and 2	2006	1-Flash	2 × 45	H.	It was initially designed as an electric generating station and then later became a cogeneration heat and power plant. Unit 3 is low pressure turbine, taking advantage of large volume of hot water from Units 1 and 2 separator. There are three separations stations with 21 water-steam separators in total	Di Pippo (2012) and Gunnlaugsson (2012)
		3	2007	1-Flash	1 × 33	H.		
		4 and 5	2008	1-Flash	2 × 45	H.		
		6 and 7	2011	1-Flash	2 × 45	H.		
Iceland	Krafla	1	1978	2-Flash	1 × 30	V.	Initially, wellhead separators were installed for each well pad. They were replaced with a centralised separation station. Due to ineffectiveness	Juliusson et al. (2005)
Iceland	Svartsengi	PP-1	1977	1-Flash	2 × 1	N.A.	The turbines are the backpressure type	Thorolfsson (2005), Albertsson et al. (2010) and Di Pippo (2012)
		PP-2	1981	–	–	–	PP-2 is not used for electricity generation. It is used for district heating with capacity 3 × 25 MWth	
		PP-3	1981	1-Flash	1 × 6	V.	The turbine is the backpressure type. The separator is located close to the turbine	
		PP-4	1989, 1993	Binary	3 × 1.2, 4 × 1.2	N.A.	It was the first time in the world an Ormat's ORC unit was directly connected to a backpressure turbine as a bottoming unit	
		PP-5	1999	1-Flash	1 × 30	H.	The steam supply system comprises a horizontal separator and a horizontal moisture separator, both with mist eliminator pads	
		PP-6	2007	Dry Steam	1 × 30	–	–	
Russia	Mutnovsky	1	2002	1-Flash	2 × 25	H.	All equipment except the two-phase pipeline is located inside the building to protect the plant equipment and personnel from the harsh winter weather. One building is used as the power house, while another building is used as a separator building	Povarov et al. (2003) and Di Pippo (2012)
Russia	Verkhne-Mutnovsky	1	1998	1-Flash	1 × 4	H.	The separated brine is flashed to be used by steam jet ejectors for non-condensable gas removal. The unique feature of this plant is the use of an air-cooled condenser normally found in a binary plant	Di Pippo (2012)
		2 and 3	1999	1-Flash	2 × 4	H.		
United States of America	Beowawe	1	1985	2-Flash	1 × 16	V., H.	The vertical separator is used to separate steam and water while the horizontal separator is used as a flasher for the hot brine produced from the vertical one	Di Pippo (2008) and Di Pippo (2012)

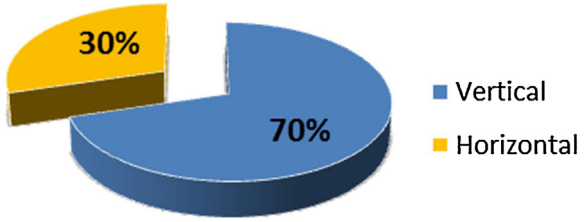

Fig. 3. The distribution of vertical separator vs horizontal separator worldwide.

nuclear industry. The horizontal separator is claimed to be superior to the vertical cyclone separator for the following reasons:

- The cyclone separation system works effectively only in designed flow regime. Deviation from this regime will affect the load and may lead to deterioration of separation effectiveness and the increase of outlet steam wetness (Povarov et al., 2003; Povarov and Nikolskiy, 2003, 2005).
- Water drop in the horizontal separator is at right angle with the steam flow, thus, creating more effective separation process than that of the vertical separator (Moghaddam, 2006).
- The horizontal separator makes access and service to the measuring equipment easier than the vertical type (Moghaddam, 2006).

Table 1 shows the separator installation in several fields across the world. Some fields (e.g. Beowawe) use a vertical separator for the high pressure and a horizontal separator for low pressure flash vessel.

4. Selection of separation pressure and specification

The separation process is simply an application of the first law of thermodynamics of heat and mass balance (Fig. 4).

Making a decision on the optimum separation pressure in geothermal power station is not straightforward. Proper understanding of thermodynamics of the conversion process is needed.

Fig. 4 shows the geothermal fluid with enthalpy h_1 and mass flow m_f undergoes flashing at constant enthalpy as it travels from the wells to the separator dropping in pressure. Inside the separator, saturated water h_3 and saturated steam h_4 are produced (Fig. 4). The steam with high enthalpy h_4 is sent to the turbine, while the liquid (brine) with enthalpy h_3 is sent to the reinjection wells. By assuming that there is no heat or pressure loss between the separator and the turbine, the inlet steam enthalpy will be equal to

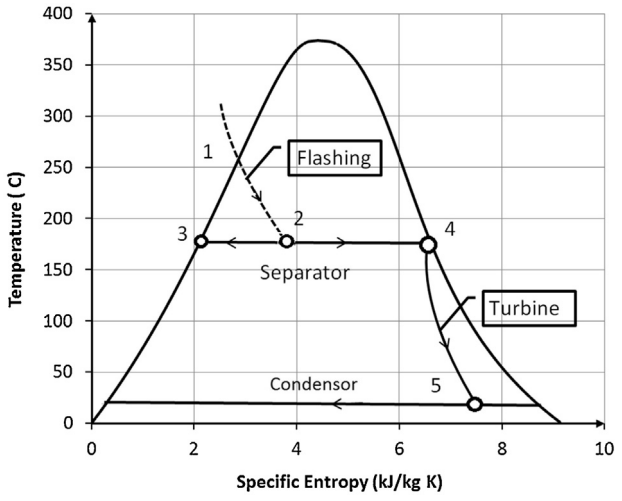

Fig. 4. Temperature entropy diagram for typical single flash plant.

h_4. Hence, the turbine gross mechanical power can be represented mathematically in the simplest form as:

$$W = \dot{m}_s \times (h_4 - h_5) \quad (1)$$

$$\dot{m}_s = \left(\frac{h_2 - h_3}{h_4 - h_3}\right) \times \dot{m}_f \quad (2)$$

where $\dot{m}_s$ is mass of steam flow rate in kg/s; h is enthalpy in kJ/kg; and W is the power in kW.

Net electrical power can be calculated by including generator efficiency in Eq. (1) after considering the effect of non-condensable gases (NCG) and parasitic load (Zarrouk and Moon, 2014).

For geothermal resource with certain mass flow rate and enthalpy, Eqs. (1) and (2) show that the produced turbine output is influenced by the separator pressure. It should be noted that the produced geothermal fluid (measured in kg/s) is usually a function of the wellhead pressure (measured in bara). In order to get the optimum turbine inlet pressure, the turbine output should be calculated for various separation pressures. The separator pressure which gives the maximum turbine output will be selected as the optimum pressure after considering any pressure losses from the separator to the turbine.

Fig. 5 indicates typical plant performance in terms of the power generation for various separation pressures. The same principle applies for double flash and triple flash plants.

4.1. Silica scaling consideration

Dissolved silica (SiO_2) is the common mineral found in geothermal fluid which can cause scaling problems in steam field equipment, especially in separators, heat exchangers, brine pipelines and reinjection wells (Zarrouk et al., 2014). Silica usually exists as amorphous silica or quartz with its own solubility characteristic. The solubility in the hot reservoir fluid is controlled by quartz (Fournier, 1986) whereas at the surface is controlled by the solubility of amorphous silica (Fournier and Rowe, 1977) (see Fig. 6).

Since silica is dissolved in liquid, as the geothermal fluid is flashed, its concentration increases in the geothermal brine due to the loss of steam. Further flashing will result in higher silica concentration in the brine, resulting in high probability of scaling problems.

To predict the probability of scaling occurrence, silica saturation index (SSI) is used. SSI is the ratio of measured silica concentration in solution to the equilibrium solubility of amorphous silica at the same pH and temperature. Saturation occurs when SSI is equal to one. When SSI is less than one, there will be less risk of silica deposition, whereas when SSI is greater than one, there will be higher risk for silica deposition.

The SSI should be considered when setting the optimum separation pressure. Based on field experience, Barnett (2007) recommended a SSI $\leq$ 1.15 for single flash and SSI $\leq$ 1.3 for double flash plants/separators. Therefore, adjustment on selected optimum pressure might be required to reduce the value of SSI and minimise scaling. If adjustment does not give significant effect, other scaling prevention techniques should be considered (e.g. acidizing).

It should be noted that silica scaling cannot be prevented 100%, but the above criteria will result in small amount/rate of scaling which is manageable. Silica scaling has been reported to take place mainly in the bottom of separators and water (brine) drums in several geothermal developments (Adiprana et al., 2010; Delliou, 1989; Grassiani, 2000; Tassew, 2001).

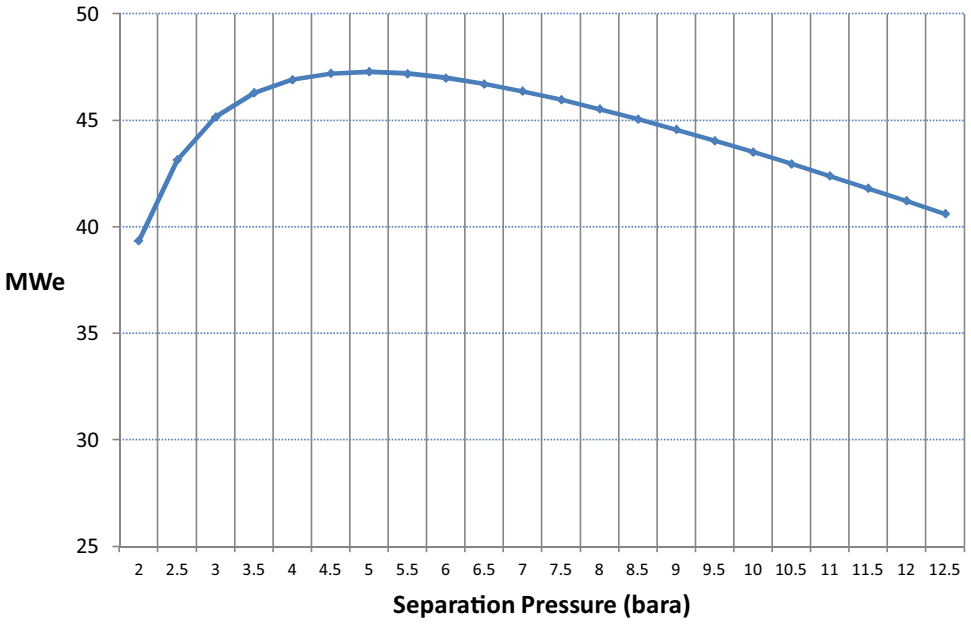

Fig. 5. Generated power vs separation pressure.

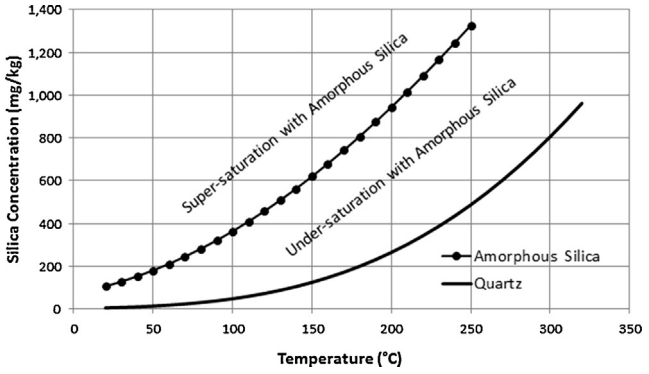

Fig. 6. Temperature dependence of the solubility of quartz and amorphous forms of silica (after, Fournier and Rowe, 1977 and Fournier, 1986).

Villaseñor and Calibugan (2011) reported silica scaling on the walls of the inlet nozzle of the separator at the Tiwi geothermal field in the Philippines.

Scaling will affect the efficiency and performance of the separator by reducing the available internal volume of the separator through the build-up of scale. This will hinder the flow of brine, reducing steam quality (increase in carry over) and can result in separator flooding. Lazalde-Crabtree (1984) recommended annual inspection and cleaning of the separator vessel.

5. Methods of separator sizing

The liquid-vapour separation process involves a combination of the following mechanisms: gravity settling, centrifugal impact, flow-line interception, diffusion deposition, electrostatic attraction, thermal precipitation, flux forces and particle agglomeration techniques (Lee, 1995). Most separators rarely operate solely with a single mechanism, although one mechanism may dominate (Lee, 1995). The vertical cyclone separator and horizontal separator work on different mechanisms. Centrifugal action is the dominant mechanism for the vertical cyclone separator, while gravity settling is the dominant mechanism for a horizontal separator.

The fluid entering the separator is a mixture of water and vapour. Understanding of two phase flow behaviour is necessary as it is strongly linked to the separation efficiency (White, 1983).

Two-phase fluid can form different flow regimes inside geothermal pipelines as shown in Fig. 7. The bubble flow is formed if there are bubbles of steam/gas that moves at approximately the same velocity as the liquid, but only at the upper part of the pipe. The plug flow is formed if there are alternating plugs of liquid and gas that move at the upper part of the pipe. The stratified flow is formed when the liquid travels at the low part of the pipe, while the gas travels in the upper side of the pipe and both are separated by a smooth liquid–gas interface. The wave flow is similar to the stratified flow but the gas moves at a higher velocity and the liquid–gas interface is disturbed by waves travelling in the flow direction. The slug flow is formed if the wave of the liquid is picked up by the more rapidly moving gas to form a frothy slug which passes through the pipe at much greater velocity than the average liquid velocity. The annular flow is formed when the gas flows at high velocity at the centre of the pipe surrounded by the film of liquid flow on the pipe walls. The mist flow is formed when most or nearly all of the liquid is entrained as spray by the gas (Harrison, 1975).

Slug flow is not desired due to the high pressure drop, vibration and its potential to create problems for the piping support. Annular flow is desirable from the standpoint of pipe restraint and low pressure drop (Darmawan, 1988). White (1983) used separator testing data from Iceland to show that for separator efficiency, better performance was obtained for inlet pipes operating in slug flow regime while annular flow regime could be associated with failure. However, typically it is not possible to alter the flow regime.

Predicting the fluid flow regime accurately is difficult. Some methods have been developed and mostly are presented in two dimensional flow pattern maps. One map that is commonly used is the Baker map (Allen, 1977) which was derived using the mass velocity of liquid and air.

For flow in geothermal pipelines, the commonly used flow pattern map is the one proposed by Mandhane et al. (1974) as shown in Fig. 8. Mandhane et al. (1974) developed the map as improvements to the previously available maps. The main advantage of this

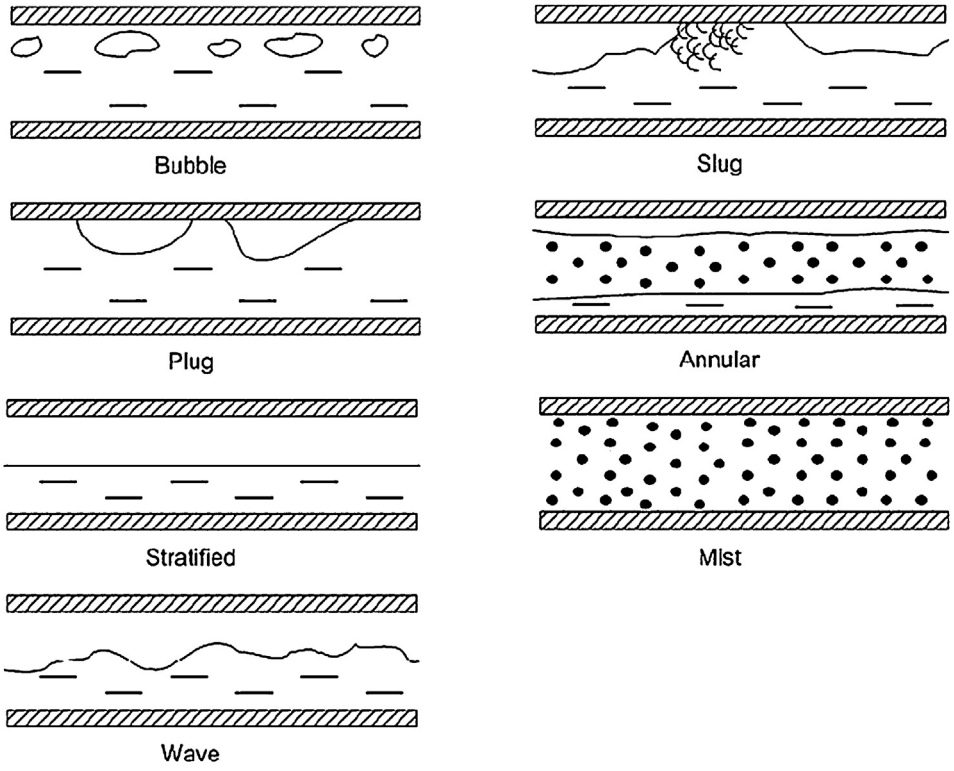

Fig. 7. Two-phase flow patterns in horizontal flow (after Harrison, 1975; Allen, 1977).

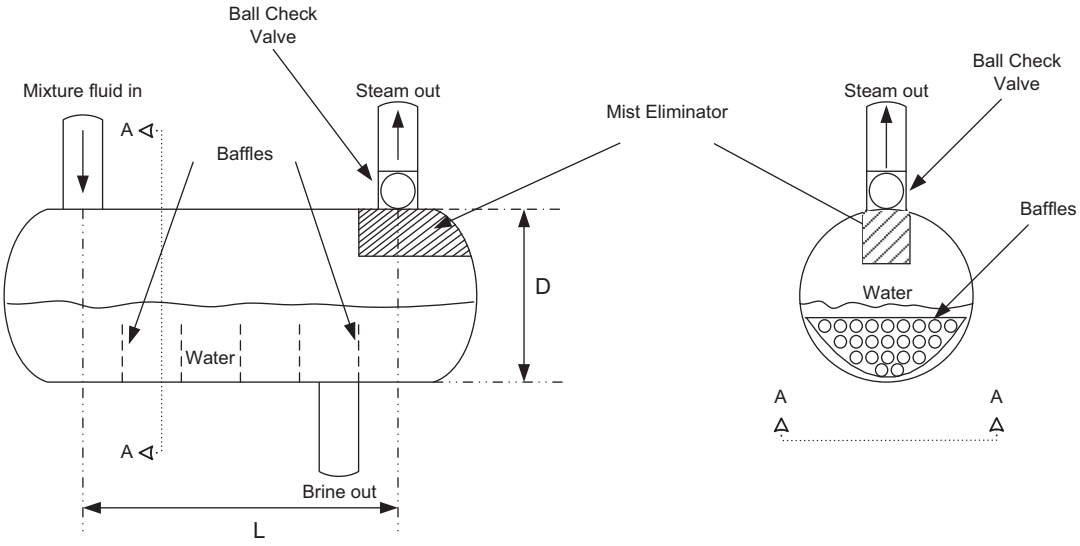

Fig. 8. Mandhane's map (after Mandhane et al., 1974).

map is its simplicity, since it is based on the superficial velocities of the two fluids. However, the map needs to be adjusted for the specific characteristics of the fluids.

Experience has shown that no single pattern map works for all ranges of pipe diameter. A new map, similar to Mandhane et al. (1974), was developed from a wider range data, but it does not perform well in pipes of larger diameters.

5.1. Sizing horizontal-type separators

Horizontal separators are mainly flash vessels where the mixture fluid enters from the first top connection of the vessel and travels horizontally while flashing occurs. Water will move downward due to gravity while steam flows from the second top connection at the opposite side of the inlet (Fig. 9). A ball check vessel is usually installed at the steam outlet to avoid water flooding the dry steam line. The chief concern is to have the mixture velocity sufficiently lowered to give the liquid particles enough time to settle before the steam leaves the vessel from the top (Gerunda, 1981).

The two parameters concerned with horizontal separator design are mixture fluid velocity and gas residence time. Both are functions of vessel diameter. Gerunda (1981) suggested that the following points should be followed:

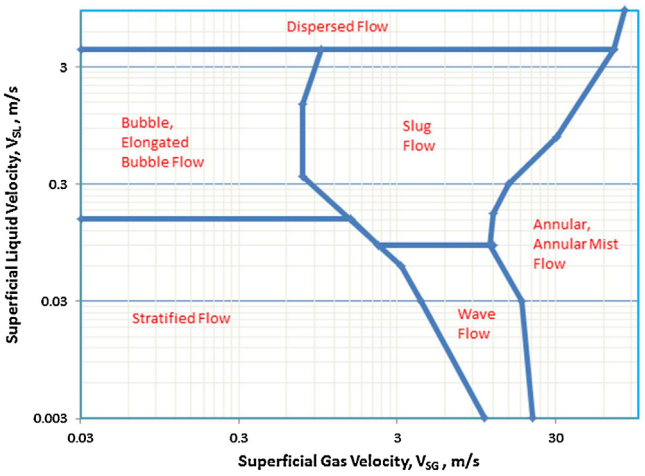

Fig. 9. Dimensions for horizontal separator (after Gerunda, 1981).

1. The maximum liquid level should not exceed 0.3 m from the top of the vessel provided that it does not drop below the centre-line of the separator.
2. The volume of vessel dished heads is not taken into account in vessel sizing calculations.
3. Inlet and outlet nozzles shall be located as close as practically possible to the vessel tangent lines.
4. Liquid outlets should have anti-vortex baffles.

Several parameters must be considered for designing a horizontal separator. The parameters are terminal velocity, vapour velocity in the horizontal direction and holding time. Gerunda (1981) proposed two approaches for the sizing of horizontal vessel; by liquid separation and by the holding time.

For a given two-phase flow, the first step is to determine the terminal velocity (v_t) as a function of liquid density (ρ_L) and vapour density (ρ_v) using Eq. (3) below. K' is a constant value based on gravity, droplet diameter and the drag coefficient of a liquid particle. For most systems, K' ranges between 0.03 and 0.012 (m/s). Gerunda (1981) recommended the value for K' to be 0.069 (m/s) except when special considerations are warranted. This value is dimensionless and should be used in Eq. (3) with the following fluid properties: ρ_l and ρ_v in kg/m^3, resulting v_t in m/s.

$$v_t = K' \left[\frac{\rho_l - \rho_v}{\rho_v} \right]^{1/2} \tag{3}$$

By calculating the gas residence time and equating it with the time required for the liquid particles to settle out at the terminal vapour velocity, Eq. (4) is obtained and can be used to set the vessel diameter.

$$D = \left[\frac{0.093 \times f_{hv} V}{(L/D)(\pi/4) f_{av} v_a} \right] \tag{4}$$

where, V is the volumetric flow rate (m^3/s); f_{hv} is the fraction of height; f_{av} is the fraction of area; v_a is the allowable vapour velocity (m/s); D is the diameter of vessel (m); and L is the length of the vessel (m).

From experience, Gerunda (1981) recommended the allowable vapour velocity (v_a) to be 15% of the calculated terminal velocity (v_t) to ensure acceptable liquid dis-entrainment during normal flow surges. However, this recommendation may be neglected (i.e. $v_a = v_t$) if the mist eliminator is installed inside the separator which results in a smaller vessel diameter.

Trial and error is required to solve Eq. (4). Gerunda (1981) proposed a general guideline for L/D ratio as given in Table 2, after considering economics and layout restrictions. Another assumption that can be made is by setting the liquid level at the centre of the separator, so that $f_h = f_a = 0.5$.

Table 2
L/D ratio for different pressure (modified from Gerunda, 1981).

Operating pressure (barg)	L/D ratio
0–17.24	3.0
17.25–34.47	4.0
34.48 and higher	5.0

When the horizontal separator size is set by holding time of the liquid, the diameter of the horizontal vessel must be determined from trial and error. To solve this problem, the following approach can be used: considering holding time (t_h) formula as given by Eq. (5), a new fraction area, f_{al}, is introduced and defined as the fraction of area occupied by the liquid. Rearranging this equation to solve for D, Eq. (6) is obtained. Using the L/D ratio from Table 2, D can be calculated.

$$t_h = \frac{(\pi/4) D^2 f_{al} L}{V_l} \tag{5}$$

$$D = \left[\frac{0.0283 \times t_h V_l}{(L/D)(\pi/4) f_{al}} \right]^{\frac{1}{3}} \tag{6}$$

where V_l is volumetric flow rate of the liquid (m^3/s), f_{al} is the fraction area occupied by the liquid, t_h is the liquid holding time (s), D is the diameter of vessel (m); and L is the length of vessel (m).

5.2. Sizing vertical-type separators

The fundamental principle of a vertical cyclone separator is to create a vortex that will centrifuge the liquid to the vessel walls, letting the steam concentrate in the middle. Under gravity, the liquid at the walls will move down and be collected at the bottom of the vessel, while the steam will enter the middle tube and will be directed to leave the vessel through the bottom pipe (Fig. 10).

Leith and Licht (1972) suggested that the efficiency of a cyclone separator depends on three dimensionless parameters: C, a cyclone design number depending upon the physical shape (not size); ψ', a modified type of impaction parameter depending upon operating condition; and n, the exponent in the modified form of the vortex law for tangential velocity distribution. Leith and Licht's (1972) approach was based on the concept of continual radial backmixing of the uncollected particles, coupled with the calculation of an average residence time for the gas in a cyclone separator having a tangential inlet. Leith and Licht's (1972) work was developed for a de-duster and later modified by Lazalde-Crabtree (1984) for a geothermal vertical cyclone separator.

Both the Bangma (1961) and Lazalde-Crabtree (1984) methods can be used to design the dimensions of the vertical cyclone separator. The vessel dimensions are all given in terms of diameter of the two-phase inlet pipe. The calculation of inlet pipe size (diameter) is given as follows:

$$A = \frac{Q_{VS}}{v_t} \tag{7}$$

$$D_t = \left[\frac{4A}{\pi} \right]^{\frac{1}{2}} \tag{8}$$

where A is the cross sectional area of the inlet nozzle/pipe; Q_{VS} is the volumetric steam flow; and D_t is the inlet pipe diameter. Fig. 10 and Table 3 show the recommended size of the vertical vessel.

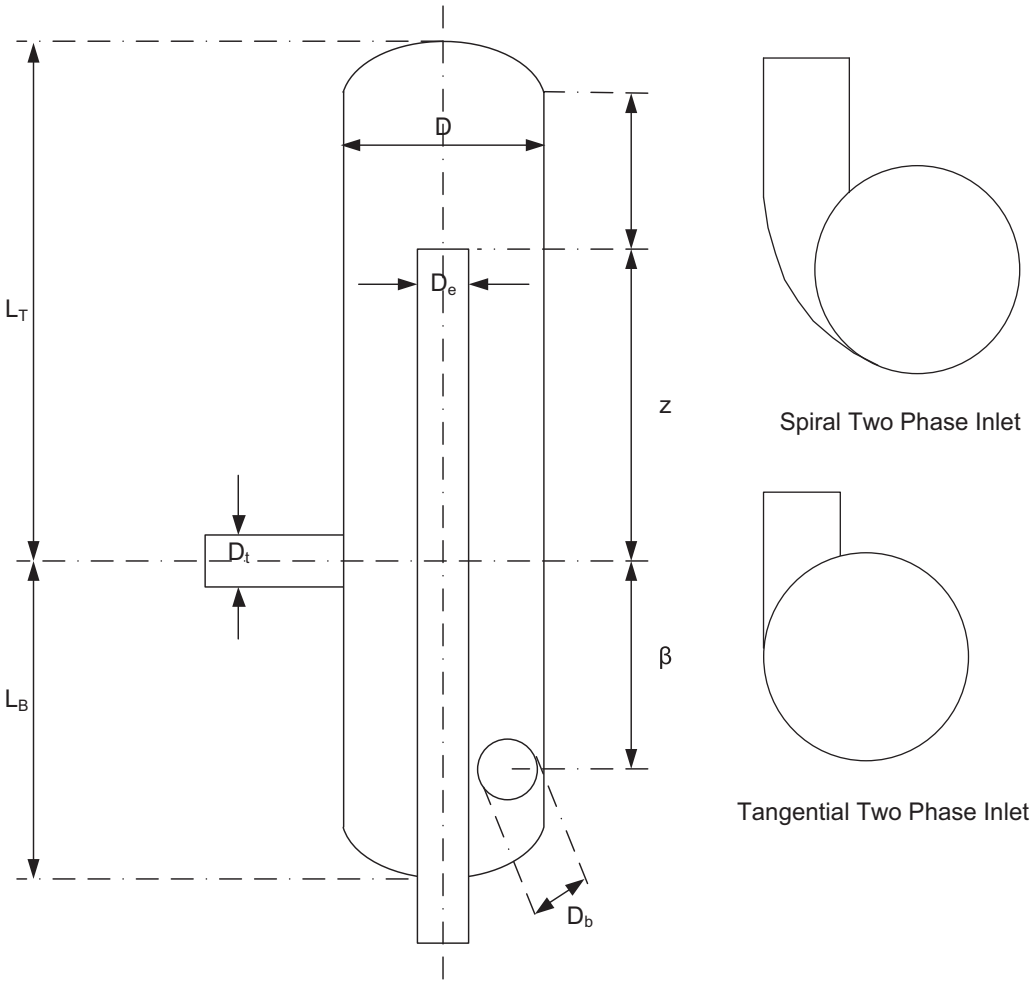

Fig. 10. Vertical BOC separator (after Bangma, 1961; Lazalde-Crabtree, 1984).

5.3. Separator efficiency

The separator performance is a measure of the proportion of brine that is carried over with the steam:

$$\eta_s = \frac{\dot{m}_s}{\dot{m}_s + \dot{m}_b} \times 100 \quad \text{or} \quad \eta_s = \frac{\dot{m}_w - \dot{m}_b}{\dot{m}_w} \times 100 \tag{9}$$

where η_s is the separator efficiency, $\dot{m}_s$, $\dot{m}_w$ and $\dot{m}_b$ are the steam flow rate, water flow rate and brine carryover (t/h or kg/s), respectively.

Table 3
Vertical bottom outlet cyclone separator dimension to be used with Fig. 10.

Parameter	Bangma (1961)	Lazalde-Crabtree (1984)
D	$3D_t$	$3.3D_t$
D_e	$0.8D_t$ [a] or $1D_t$ [b]	$1D_t$
D_b	$1D_t$	$1D_t$
α	$3D_t$	$-0.15D_t$ [c]
β	$3D_t$	$3.5D_t$
Z	$3D_t$ [a] or $4D_t$ [b]	$5.5D_t$
L_T	$7D_t$	$\approx 6D_t$
L_B	$4.5D_t$	$>4.0D_t$
A_o	Circle; $A_o = \frac{1}{4}\pi D_t^2$	Rectangle; $A_o = A_e \cdot B_e$

D_t is inlet pipe diameter.
[a] Tangential inlet.
[b] Spiral inlet.
[c] The negative sign implies it is up in the domed end.

Typical efficiency ranges between 99.5% and 99.99%. However, practical experience has shown that, a perfect 100% efficiency ($m_b = 0$) should not be expected.

It is not practically possible to directly measure the brine carryover ($\dot{m}_b$) to calculate the separator efficiency (Eq. (9)). This is because it is a small component of steam flow and also it is masked (diluted) by condensate forming in the steam pipeline as the pipelines lose heat. However, the carryover can be measured indirectly using the chemical signature of the geothermal brine namely Sodium (Bangma, 1960) other natural tracers like Chloride can potentially be used. The principle is that carryover from the separator introduces sodium into the steam pipelines. Measuring the concentration of sodium in the separated steam can be used to calculate the brine carryover:

$$\dot{m}_b = \frac{\dot{C}_S^{Na}}{C_{sb}^{Na}} \tag{10}$$

where $\dot{C}_s^{Na}$ is the mass flow rate of sodium in the separated steam in mg/s and $\dot{C}_{sb}^{Na}$ is the concentration of sodium in separated brine in mg/kg.

White (1983) proposed a similar equation for calculating separation efficiency from the ratio of outlet purity to the inlet purity, where steam purity is defined as the total dissolved (TDS) solids in the steam. The correlation can be shown as follows:

$$Sp = \dot{m}_b \times \text{TDS} \quad \text{or} \quad Sp = \frac{\dot{C}_s^{Na}}{C_{sb}^{Na}} \times \text{TDS} \tag{11}$$

$$\eta_s = \left[1 - \frac{\dot{C}_s^{Na}}{C_{sb}^{Na}}\right] \times 100 \quad (12)$$

where TDS is the Total Dissolved Solids in the brine (ppm), *Sp* is the separated water purity (mg/s).

The natural tracer concentration is normally measured in the drain pot following the separator. Note that isokinetic probes normally installed near the power station may not be suitable for sampling of sodium due to low sodium concentration by the time the steam reaches the station. This is due to scrubbing effects in multiple drain pots and/or potentially injection of wash water if large scrubbers near the power stations are used.

However, the chemical tracer method can only be used once the separators have been built and put into operation to determine the actual performance.

The most popular empirical approach to estimate the efficiency of a geothermal vertical cyclone separator is the one proposed by Lazalde-Crabtree (1984). Lazalde-Crabtree (1984) defines the separator (theoretical) efficiency as a product of centrifugal efficiency and entrainment efficiency.

$$\eta_{eff} = \eta_m \cdot \eta_A \quad (13)$$

where η_{eff} is the effective efficiency; η_m is the centrifugal efficiency; and η_A is the entrainment efficiency.

Foong (2005) effectively related the difference between the theoretical efficiency (η_{eff}) and the actual efficiency (η_S) to water creep along the vessel walls.

The centrifugal efficiency (η_m) that reflects the operating condition inside the cyclone is strongly influenced by the diameter of drop particles (d_w) and the tangential inlet velocity of the steam (u) as given in Eqs. (14)–(21) below:

$$\eta_m = 1 - exp\left[-2(\psi' C)^{\frac{1}{2n+2}}\right] \quad (14)$$

where C is a dimensionless parameter given by Eq. (19); n is a dimensionless free vortex law coefficient given by Eq. (20) and ψ' is the centrifugal inertia impaction parameter given by Eq. (21).

$$C = \frac{8K_c D^2}{A_o} \quad (15)$$

$$\frac{1-n_1}{1-n} = \left(\frac{294.3}{T+273.2}\right)^{0.3} \quad (16)$$

where K_c is a dimensionless parameter given by Eq. (17), A_o is the inlet shape area; T is the saturated temperature; n is a parameter determined from Eq. (16) when $n_1 = 0.6689\ D^{0.14}$.

$$K_c = \frac{t_r Q_{VS}}{D^3} \quad (17)$$

where t_r is the residence time, obtained from the following equation:

$$t_r = t_{mi} + \frac{t_{ma}}{2} \quad (18)$$

where t_{mi} is the average minimum residence time of steam inside the vessel and t_{ma} is the maximum additional time of steam inside the cyclone as given by Eqs. (19) and (20), respectively.

$$t_{mi} = \frac{V_{os}}{Q_{VS}} \quad (19)$$

$$t_{ma} = \frac{V_{OH}}{Q_{VS}} \quad (20)$$

Table 4
Variables *a*, *B*, *e* used with Eq. (23) (from Lazalde-Crabtree, 1984).

Type of 2-phase flow pattern	*a*	*B*	*e*
Stratified and wavy	0.5436	$94.9042\ (X_i)^{-0.4538}$	0.0253
Annular	0.8069	$198.7749\ (X_i)^{0.2628}$	−0.2188
Dispersed and bubble	0.8069	$140.8346\ (X_i)^{0.5747}$	−0.2188
Plug and slug	0.5436	$37.3618\ (X_i)^{-0.0000688}$	0.0253

where V_{OS} and V_{OH} are the volume of steam inside the vessel given by Fig. 11.

The centrifugal inertial impaction is very sensitive to the droplet diameter as shown in Eq. (21) below:

$$\psi' = \frac{\rho_w d_w^2 (n+1) u}{18 \mu_v D} \quad (21)$$

where μ_v is the steam viscosity and u is the inlet steam velocity derived from Eq. (22).

$$u = \frac{Q_{VS}}{A_o} \quad (22)$$

Determination of the drop particle size was given by Lazalde-Crabtree using the basic equation developed by Nukiyami–Tanasawa combined with the data obtained from actual well-head separators (Lazalde-Crabtree, 1984). Lazalde-Crabtree's (1984) final formula is given by Eq. (23).

$$d_w = \frac{66.2898}{v_t^a}\sqrt{\frac{\sigma_L}{\rho_L}} + B.(1357.35)\left[\frac{\mu_L^2}{\sigma_L \rho_L}\right]^{0.2250} \times \left(\frac{Q_L}{Q_{VS}}\right)^{0.5507} \times v_t^e \quad (23)$$

Eq. (23) should be used with the following dimensions: ρ_L in g/cm^3, v_t in m/s, σ_L in dyne/cm, μ_L in poise, Q_L and Q_{VS} in m^3/s, resulting in d_w in microns. The variables *a*, *B*, and *e* are dependent on the type of two-phase flow regime according to Baker's map and are given in Table 4.

To calculate the surface tension of water as function of temperature, the following approach can be used (Vargaftic et al., 1983):

$$\sigma = Y\left[\frac{T_c - (T+273.15)}{T_c}\right]^k \times \left[1 + b\left(\frac{T_c - (T+273.15)}{T_c}\right)\right] \quad (24)$$

where $T_c = 647.15$ K; $Y = 235.8 \times 10^{-3}$ N/m; $b = -0.625$; $k = 1.256$; resulting in σ in N/m.

The entrainment efficiency (η_A) is function of annular steam velocity given by Eqs. (25)–(27).

$$\eta_A = 10^j \quad (25)$$

$$j = -3.384(10^{-14})(V_{AN})^{13.9241} \quad (26)$$

$$V_{AN} = \frac{4Q_{VS}}{\pi(D^2 - D_e^2)} \quad (27)$$

where the range of η_A should be $0 \le \eta_A \le 1$.

The pressure drop can be expressed as:

$$\Delta P = \frac{(NH)u^2 \rho_v}{2} \quad (28)$$

$$NH = 16\frac{A_o}{D_e^2} \quad (29)$$

where ΔP is the steam pressure drop; u is the tangential inlet velocity; ρ_v is the density of vapour; A_o is the inlet shape area; and D_e is the steam outlet pipe diameter.

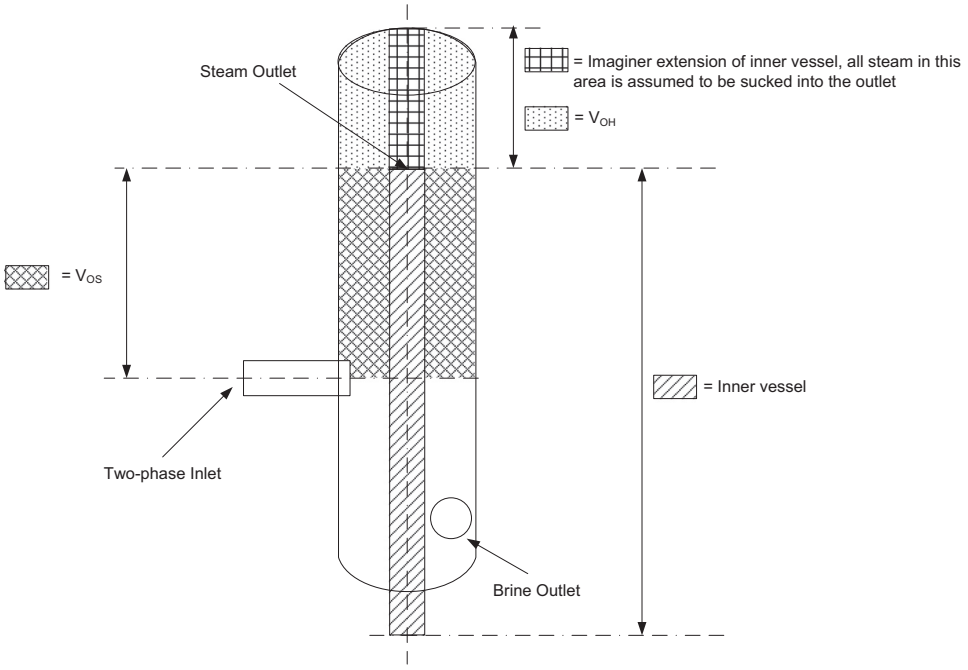

Fig. 11. VOS and VOH calculation (from Lazalde-Crabtree, 1984).

5.4. *Effect of inlet nozzle design on BOC separator performance*

The cross section of the cyclone separator inlet can be circular, square or rectangular. A circular inlet is simple in construction due to the fact that the two phase pipe can be used directly as the entry point of the cyclone separator. In contrast, a rectangular inlet requires a circular to rectangular transition piece, located fairly close to the cyclone body. Design of this transition piece must be performed carefully to create a smooth transition process. Improper design might lead to boundary layer separation and extra turbulence in the incoming flow (Hoffmann and Stein, 2007).

The early circular spiral inlet nozzle design was tested in Wairakei, New Zealand in late 1950s (Bangma, 1960). The nozzles were made of cast steel with an effective transition (downward slope) from circular section to rectangular section as the pipe joins the body of the separator. This downward slope was further increase/improved in the more recent designs and the transition from circular section to square or rectangular sections is taking place further outside the separator body. The rectangular inlet is preferred by some designers as it joins the body of the cyclone more smoothly.

The quality of separation for vertical BOC separator is influenced by the inlet flow conditions. As the inlet velocity increases, the output steam wetness is essentially flat until it reaches a certain point where the output steam wetness increases drastically (Lazalde-Crabtree, 1984). This point is called the breakdown velocity and is shown in Fig. 12 which demonstrates that the breakdown velocity is approximately 42 m/s (Lazalde-Crabtree, 1984). As the inlet velocity reaches this point, the outlet steam quality suddenly decreases rapidly. However, data from the early testing of the spiral inlet separator on wells WK 30 and WK 44 at Wairakei, New Zealand (Bangma, 1960) clearly show higher breakdown velocities (Fig. 12). The difference between the two studies is that (Bangma, 1960) work was carried out using a 0.76 m diameter separator while the work of Lazalde-Crabtree (1984) was based on data from a 1.4 m and/or 2.1 m diameter separators. The larger diameter separator will have a larger film of liquid flow (water creep) on the separator vessel wall, which might impact the breakdown velocity. Therefore: the calculations given in Sections 5.2 and 5.3 "*has not been tested exhaustively; therefore it should be taken only as a good procedure*" (Lazalde-Crabtree, 1984).

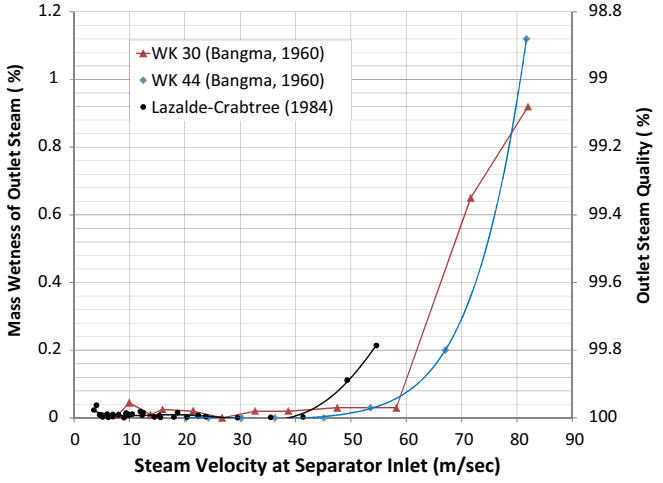

Fig. 12. Separator performance (data from Lazalde-Crabtree, 1984 and Bangma, 1960).

The highest efficiency is achieved when the inlet velocity is between 30 m/s and 40 m/s for the Lazalde-Crabtree (1984) data. However, Fig. 12 also shows that for smaller diameter separators the inlet velocity can range from 25 m/s to 45 m/s. The other challenge that arises is how to keep the inlet velocity within these ranges and just below the breakdown velocity in order to achieve the highest possible efficiency. Controlling the fluid velocity exactly at the entrance of the vessel with minimum disturbance to the incoming fluid is not practical. Hence, the only method is by designing the inlet shape geometry in such a way that the fluid velocity at the upstream pipe will remain the same as the velocity at the entrance of the cyclone body.

There are two types of separators inlet: tangential inlet and spiral inlet. The spiral inlet is superior as it provides a smoother aerodynamic transition resulting in improved separation efficiency (Hoffmann and Stein, 2007; Pointon et al., 2009). In addition, the

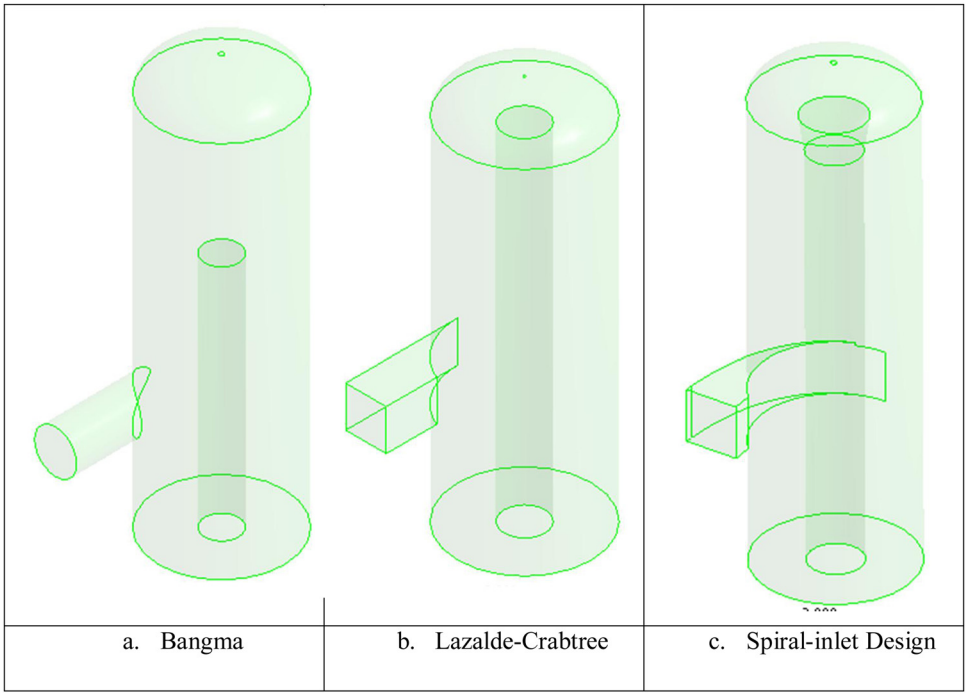

Fig. 13. Separator geometry based on (a) Bangma (1961), (b) Lazalde-Crabtree (1984), and (c) spiral-inlet.

scroll inlet produces an effect upon cyclone performance which is similar to that produced by increasing the body diameter. This brings about an increase in incoming angular momentum (Hoffmann and Stein, 2007).

6. Computational fluid dynamic (CFD) modelling of vertical cyclone separators

Unlike the results from empirical models in Sections 5.2 and 5.3 above, the CFD simulation results permit direct visualisation and quantitative interrogation of the solution results. This allows the designer to investigate flow behaviour in specific regions and to identify areas for further optimisation.

Simple analytical and numerical solutions for predicting the flow within a geothermal separator have been presented by McKibbin (1998). McKibbin (1998) was able to show a simplified model for the flow of the steam phase inside the vessel to give the flow and pressure distribution patterns.

A study using CFD software for a geothermal vertical cyclone separator design was performed by Pointon et al. (2009). Pointon et al. (2009) used the commercially available software package Fluent^{TM}, for their work. They were able to show that CFD can be used to examine particular aspects of separator design, including upstream piping arrangements, separator geometric proportions, performance of large separators and enhancements to the entry to the steam outlet tube.

Following the study of Pointon et al. (2009), Purnanto et al. (2012) conducted a similar CFD modelling study to simulate the two phase fluid movement inside a geothermal cyclone separator using Fluent^{TM}. Three different Bottom Outlet Cyclone (BOC) designs are considered. The first is according to the approach from Bangma (1961) with circular tangential inlet shape (Fig. 13a). The second is according to Lazalde-Crabtree (1984) with rectangular tangential inlet shape (Fig. 13b). The third follows the typical current separator design used in the geothermal industry with a rectangular 90° spiral inlet (Fig. 13c) which was considered to be the optimum design combination of Bangma's approach and Lazalde-Crabtree's approach. For simplicity, the typical current design will be referred to as the spiral-inlet design. In this design (Fig. 13), the steam pipe is placed inside the vessel and steam exits from the bottom of the vessel. The results were then compared and contrasted.

The model is based on a typical geothermal separator installation with a total mass flow of 200 kg/s, initial enthalpy of 1600 kJ/kg and separation pressure of 11.2 bara. Higher and lower enthalpies were also investigated to simulate changing conditions that are commonly observed during the operation of the steam field. Focus was given to the steady state condition of the two phase flow at the inlet and inside the vertical cyclone separator. The pre-separation process that occurs in the pipeline was not modelled. The flow of water to the brine pipe at the bottom of the vessel was also not modelled. The water level was assumed to be constant, located at just above the brine outlet pipe.

A suitable turbulence model provided by Fluent^{TM} was selected to model the swirling flow with high degree of turbulence. Some simplifications were made to minimise the complexity of the model.

The efficiency of the separator is predicted by using a particle tracking method. This method has been used by other researchers with the assumption that mist or mist-annular flow conditions exist at the upstream pipe feeding the separator (Hoffmann and Stein, 2007; Pointon et al., 2009; Shalaby, 2007). Separation efficiency is obtained by taking the ratio between the numbers of fine liquid droplets escaped from the steam outlet with the total number of liquid droplets at the two-phase inlet.

Considering that it is almost impossible to predict the flow behaviour and measure the droplet size distribution that is formed in the upstream pipe entering the separator, we used the Harwell technique to get a rough estimation of the average drop size. The Harwell procedure is one of several correlations available for computing drop sizes and was developed on the basis of steam-water, air–water and other fluid data (Hoffmann and Stein, 2007).

6.1. Velocity profile

The velocity vectors, coloured by velocity magnitude, for $h = 1600$ kJ/kg are shown in Fig. 14. The vectors show the spiral movement when the fluid enters the separator body. Initially, the

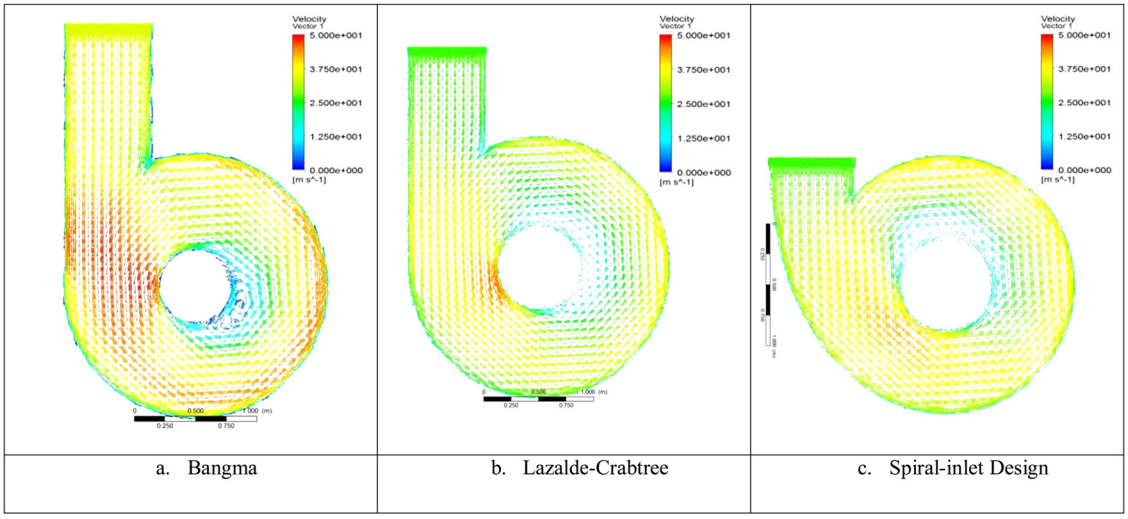

Fig. 14. Velocity profile for (a) Bangma (1961), (b) Lazalde-Crabtree (1984), and (c) spiral-inlet.

fluid enters the vessel at a particular velocity and slightly accelerates before it starts to rotate. Then, the velocity decreases as the fluid starts to rotate and follow the inner vessel wall. High velocity occurs near the outer wall of the vessel while lower velocity values occur near the centre of vessel. Similar velocity distribution was demonstrated by White (1983) when using three methods/data sources.

An interesting pattern is observed in the spiral-inlet design (Fig. 14c). The fluid enters the separator in a smooth way such that the velocity magnitude inside the vessel is relatively uniform at the first rotation. High velocity regions occur uniformly close to the outer wall, while slower moving fluid is concentrated near the centre. This condition is expected during the centrifuging process as the water will be forced to the outer vessel wall before it is affected by the steam stream in the centre of the cyclone that moves upward. Hence, the water will have a greater tendency to move downwards to be collected at the bottom of the separator.

The Bangma (1961) and Lazalde-Crabtree (1984) designs with tangential inlet shape show different patterns, where there is a region near the outer wall which has lower velocities. This indicates that the transition from linear motion into rotation is not as smooth as observed in spiral inlet design. Disturbances may create atomisation of the water as an impact of the main body of the water to the wall of the separator at a location opposite the inlet. This atomised water might be carried over by the steam, resulting in an increase of the steam wetness at the outlet of the separator.

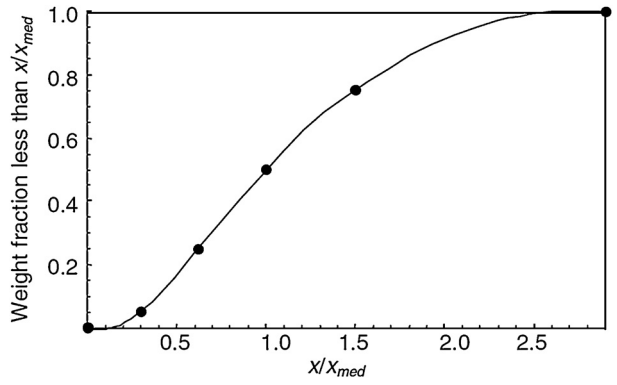

Fig. 15. Pressure distribution inside the separator at an inlet fluid enthalpy of 1760 kJ/kg for (a) Bangma (1961), (b) Lazalde-Crabtree (1984), and (c) Spiral-Inlet.

6.2. Pressure distribution profile

Fig. 15 shows the pressure distribution inside the separator in each design. Uniform patterns are found. Lower pressure is observed in the centre of the separator, while higher pressure is observed at the outer wall. This is due to the influence of cyclonic flow and the centripetal acceleration induced by the rotation (McKibbin, 1998). The advantage of this condition is that more flash may occur because of the pressure is lower than that at the fluid saturation temperature, creating a much drier steam at the outlet of the separator.

6.3. Outlet steam quality

The strategy for predicting the outlet steam quality of the separator was to inject a large number of particles at the inlet. The particle sizes were calculated using the Harwell technique (Fig. 16) and were considered to be uniformly distributed at the inlet surface. Injections were carried out nine times. Each injection used a different droplet diameter.

Although the number of injected particles for each cycle was the same, they represented different mass flow. The steam output quality was calculated as the mass flow ratio of the separated steam with the total steam-water that left from the outlet. Any droplets that reached the bottom of separator were considered to be perfectly separated.

During injection, a particle was assumed to be smooth. The maximum number of Euler time steps of 10^5 was set. After injection, there were three conditions of particles: trapped, escaped and incomplete. Trapped particles are the liquid droplets that are separated, escaped particles have been carried over to the steam outlet, while the incomplete particles have exceeded the maximum number of steps and the solver abandoned the trajectory calculation. The number of incomplete particles made the interpretation process difficult because they might be either trapped or have escaped. Increasing the maximum number of steps to be 10^6 did not significantly decrease the number of incomplete particles. It is likely that a further mesh refinement study is needed to isolate physical phenomena from numerical phenomena (e.g. numerical dispersion, etc.).

In order to cope with this problem, a possible approach was to assume that the incomplete particles were all separated.

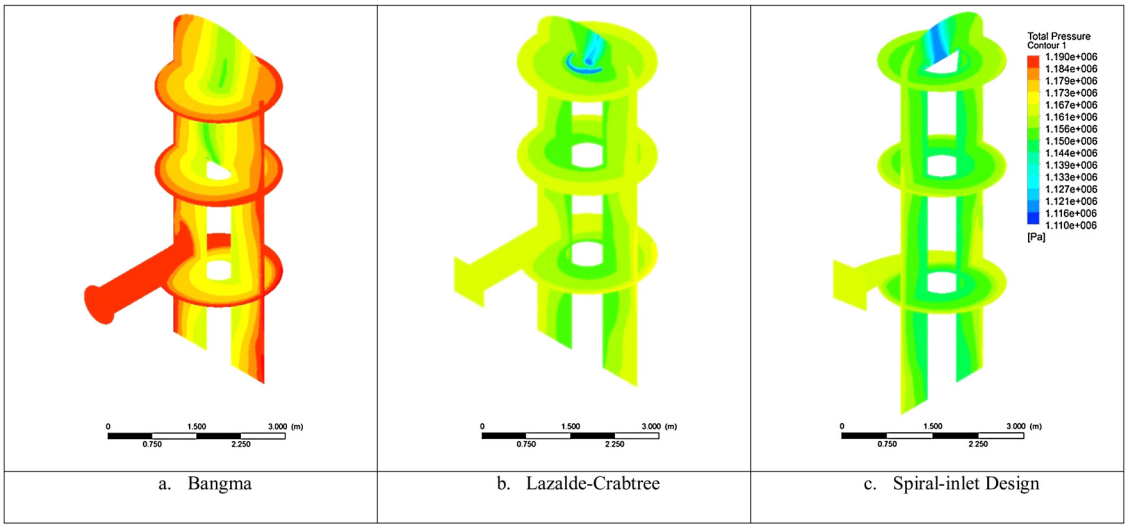

Fig. 16. Standard size distribution for droplets in pipelines (after Hoffmann and Stein, 2007).

Although this approach is not rigorous, it did provide the most promising collection efficiency estimates, close to the result from the empirical method developed by Lazalde-Crabtree (1984).

Figs. 17–19 show the differences between modelling and calculation for the different inlets types, and how the change in enthalpy and mass flow affect the outlet steam quality. The Lazalde-Crabtree's data (1984) that correlate the inlet steam velocity and the outlet steam quality are also plotted. These data were taken from several Weber separators at different geothermal fields and they were intended to show the general patterns observed in actual condition (green line).

The lowest inlet velocity corresponds to a condition when the inlet enthalpy is 1600 kJ/kg and the inlet mass flow decreases by 25%. The highest inlet velocity corresponds to a condition when the enthalpy is 1760 kJ/kg. The remaining cases are located between these two values; a low velocity value is at the left hand side while a high value is at the right hand side.

In Bangma's design (Fig. 17), the difference between calculation and simulation varies between 0.03% and 0.18%. Fig. 17 shows that the outlet steam quality increases as the inlet enthalpy increases. High outlet steam quality is also observed when the enthalpy remains the same (1600 kJ/kg) but the mass flow decreases. The simulation patterns do not follow the patterns from calculation and Lazalde-Crabtree's recorded data. Further improvement to the current model is needed to reduce with numerical dispersion and improve the CFD modelling results.

In Lazalde-Crabtree's design (Fig. 18), the difference between calculation and simulation varies between 0.02% and 0.15%. Similar to Bangma's, the output steam quality increases as the enthalpy and velocity increases (Fig. 18). The highest output quality is observed when the enthalpy is 1680 kJ/kg and the inlet velocity is 29.48 m/s. Increasing the enthalpy further will cause a slight decrease in the output steam quality.

In the spiral-inlet design (Fig. 19), the difference between simulation and calculation varies between 0.03% and 0.13%. Unexpected

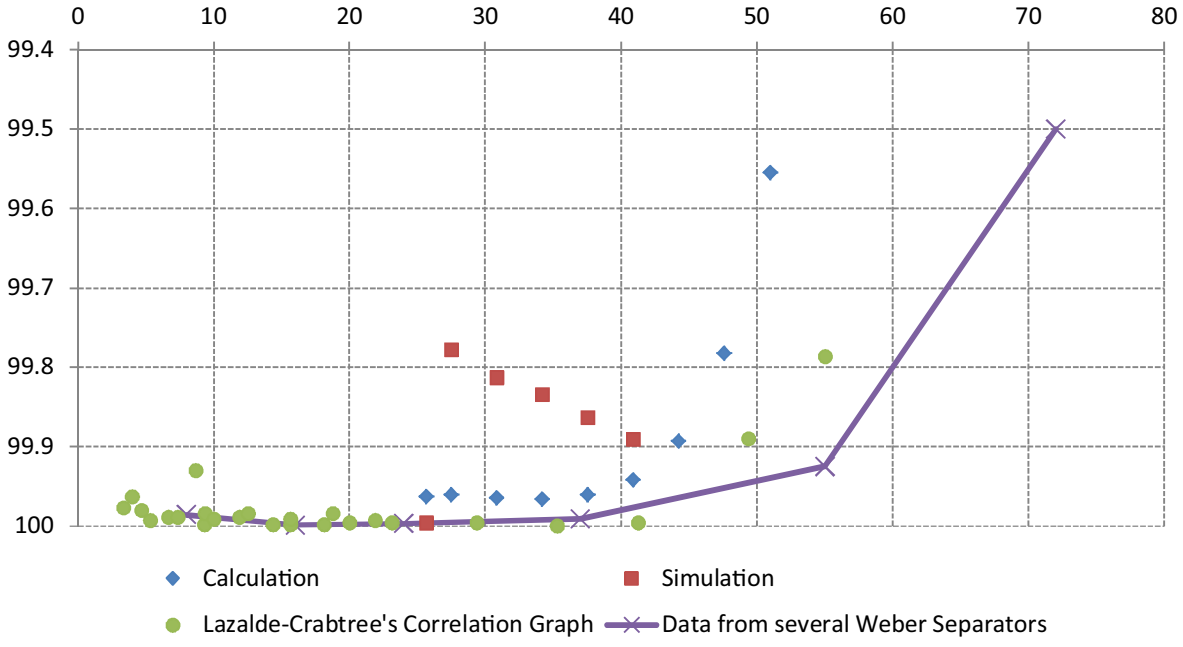

Fig. 17. Outlet steam quality against inlet velocity for the Bangma (1961).

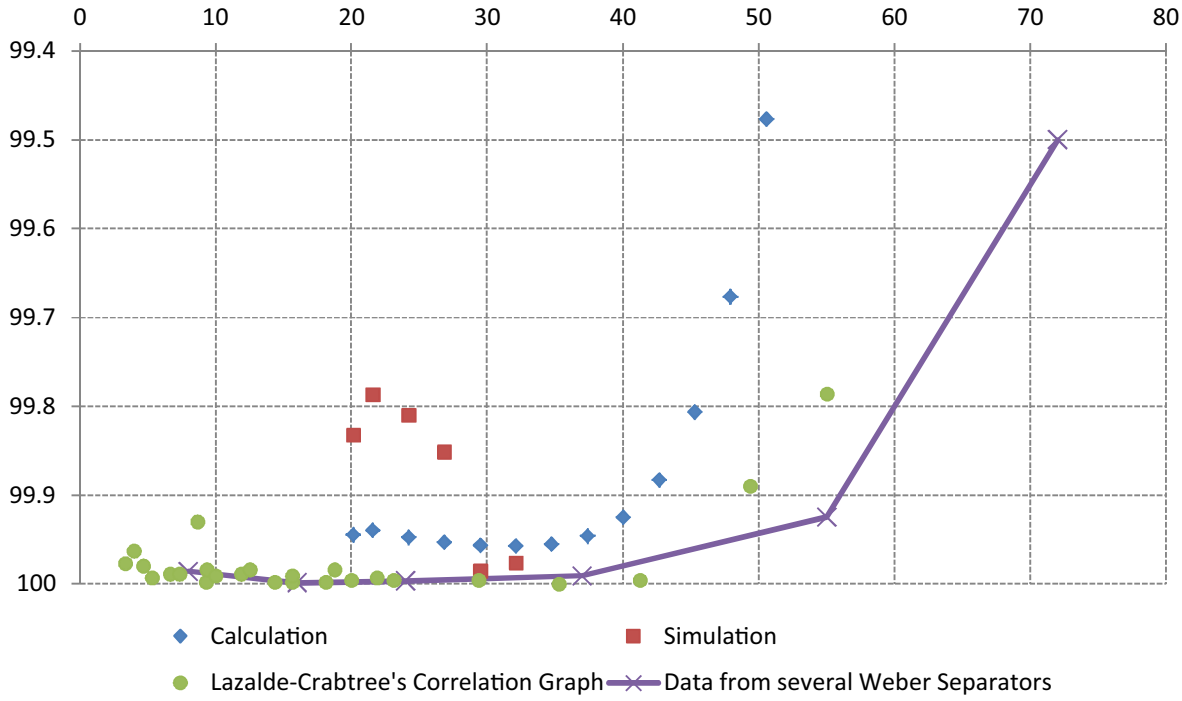

Fig. 18. Outlet steam quality against inlet velocity for the Lazalde-Crabtree (1984).

behaviour is observed when the enthalpy is 1600 kJ/kg and the inlet velocity is 27 m/s. The outlet steam quality does not follow the pattern where the quality should increase as the inlet velocity increases. The cause of this behaviour is unknown and should be further investigated.

Figs. 17–19 demonstrate that the CFD modelling is able to show how different geometry, different inlet shapes and different inlet fluid characteristics affect the separator performance. However, experimental work is still required to calibrate the result of the present CFD modelling in order to have more confidence in the results.

7. Design considerations

7.1. Separator location

The early separators in Wairakei were located at each well-head, this was mainly because geothermal two-phase flow was not well understood and because the early TOC and BOC separators designs were focused on small 30 in. (0.76 m) diameter separators (Bangma, 1960). However, this design resulted in the need for more separators, valves, longer pipelines with higher pressure drop and higher initial and maintenance cost. The following generation of steam

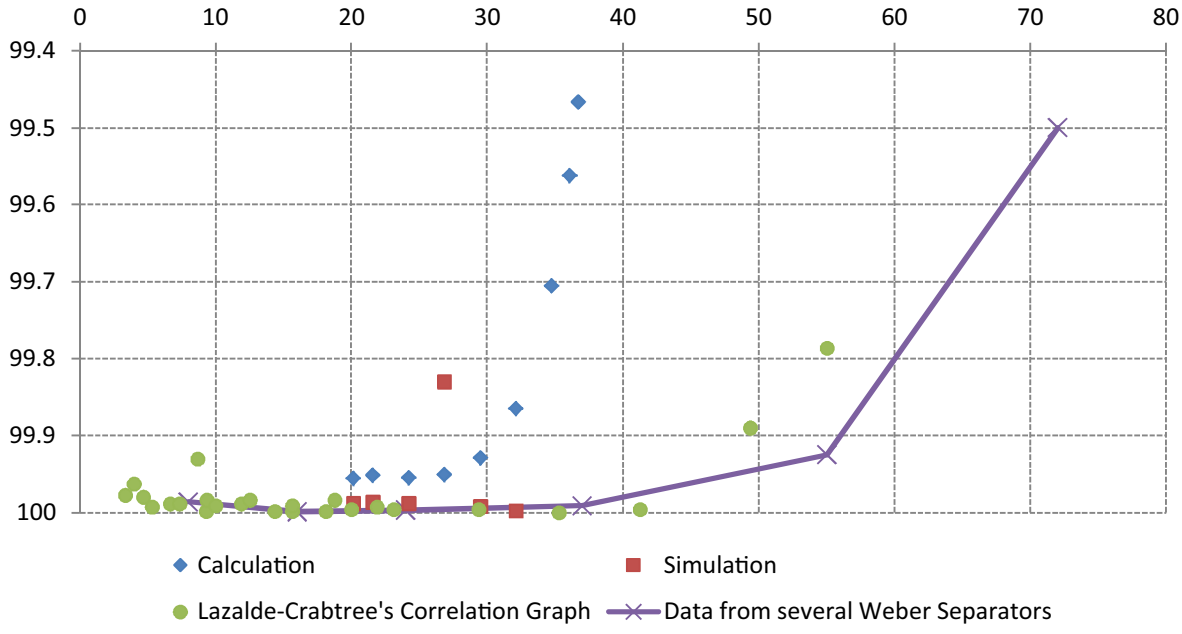

Fig. 19. Outlet steam quality against inlet velocity for the spiral-inlet.

field design (e.g. Ohaaki) implemented satellite separation stations in which two-phase geothermal fluid from several wells is collected at few satellite separation/flashing stations within the field and the steam is sent to the power station, while the separated brine is reinjected mainly infield. The latest design concept involves large centralised separators (mainly one or two) near the power station (Nga Awa Purua, Rotokawa, Mokai Te Huke, Ngatamariki) where fluid from all the wells in the field is collected and separated and possibly flashed once or twice to produce more steam.

While the well-head and satellite separators are located in the field resulting in longer pipeline runs to the power station. This will allow good scrubbing of solid minerals from separator carry over as well as good moisture removal of condensates through drain pots (Lee, 1982). It will also reduce the need for using large scrubbers and steam demisters or vortex separators (Lee, 1995) near the power stations. If the centralised separators are located close to the power station which results in shorter steam pipelines to the power station. This will mean cheaper system that is easy to control and has a lower pressure drop. However, this will make it necessary to have large scrubbers and demisters near the power stations to improve the purity and quality of the steam entering the turbine.

Having those large centralised separators near the power stations have limited the number of drain pots on the steam pipelines resulting in less time for scrubbing any carried over minerals. The large separators also meant more fluid mass entering the separator so for a maximum possible separator efficiency of 99.99% (in theory) there is significant carry over near the power station.

Since the scrubbers and demisters are not 100% efficient (Lee, 1995), there will be a carryover of water (with dissolved minerals) into the turbines which can result in both solid deposition (precipitation) on the nozzles and the early stages of the turbine blades or significant water erosion of the fixed and moving turbine blades. Several such cases have been witnessed lately in several new power stations (author's experience). This highlights the need to reconsider implementing centralised separation systems and allow more efficient deep drain pots (Lee, 1982) between the separator and the turbine (Lee, 1995). This will allow a good scrubbing of the carried over solid minerals and higher steam quality at the power station. Also having the power station at higher elevation to the steam field will result in less steam condensates flowing from the field to the station (e.g. Ohaaki and Poihipi). However, it should be kept in mind that at higher steam velocity the steam condensates can travel in the same direction as the steam. Experience at Wairakei has shown that good drain pot design is more important for a very high steam quality at the power plant.

Another important consideration when choosing the location of the separator is to prevent flashing in the separated water (brine) pipelines (Watson et al., 1996). This can take place when there is a sudden pressure drop in the reinjection/brine line causing flashing which can result in a flooding of the separator and turbine damage when water inters the turbine. On the other hand the collapse of this bubble due to steam condensation can cause pipe and valve failure (Watson et al., 1996). Measuring the flow rate of the brine leaving the separator using a pressure differential device (e.g. orifice plate) is therefore not recommended as it result higher pressure drop increasing the risk of brine flashing.

7.2. Other design features

An important requirement for separator design is the pressure drop within the vessel. Good separator design will have low pressure drop which will result in lower enthalpy loss. Hence, more energy is sent to the turbine. The BOC separator has a lower pressure drop (Eqs. (28) and (29)) compared with the TOC (Fig. 2) and earlier combined U-bend – TOC design shown in Fig. 1. However, it should be noted that the pressure drop in the horizontal separator can be less than that of the BOC, which may have influenced separator selection by some people.

The brine leaving the separator (outlet) is normally connected to a water drum (pressure vessel) immediately after the separator to help control water level inside the separator, to help form a seal against steam loss and help dampen flow/pressure surges. The water drum can be either vertically or horizontally mounted next to the separator. Early well-head separators (e.g. Wairakei) had a small horizontal water drum connected to it (Fig. 1). As the separator size increased, vertical water drums were used which gave more water level control (e.g. Wairakei and Ohaaki). Later as the separators became more centralised and larger in size, large horizontal water drums were used (e.g. Mokai, Rotokawa, Te Huka, New Zealand). Some of the more recent separators designs use built-in (integral) water storage by extending the height of the separator (e.g. the 159 MWe Te Mihi power station, New Zealand) or having the lower section of the separator larger in diameter than the upper section (e.g. the 140 MWe Nga Awa Purua power station, New Zealand). It should be pointed out that the built-in water drum was first introduced by Bangma (1960) using 48 in. (1.22 m) BOC separator. There is also a design that utilises a loop-seal to control the water level (e.g. the 227 MWe Wayang Windu, Units 1 and 2, Indonesia). In this design, the water will fill in the properly sized U-bend brine outlet pipe and become the seal between the two phase fluid and the water.

The detailed mechanical design of the separator is outside the scope of this work, but it mainly follows pressure vessel design standards. However, main features include: the separator body should be robust for handling vibration and slugging flow, minimum of 3 mm corrosion/erosion allowance (~0.1 mm/year) on the steel walls thickness, lifting and handling mounts, external water level gauge (below two-phase inlet) and manholes for access during cleaning. The separator vessel requires deep foundation to support its lateral load that results from seismic events or slug flow. It is also not allowed to move due thermal expansion in the pipeline network.

The separators are thermally insulated with fibreglass or calcium silicate to minimise heat loss and the condensation of steam which can cause drop in efficiency. The insulation material is normally covered in aluminium cladding to contain and protect it from rain and other weather elements.

Several authors have proposed or developed new separator designs including:

Jung and Wai (2000) who developed a Boundary Layer Inline Separator Scrubber (BLISS), which is horizontal multi-positional centrifugal separator, which can save 50% in cost and 75% in the overall pressure drop. This design is relatively similar in concept to the vortex separator given by Lee (1995) A horizontal in-line centrifugal separator was trialled at Wairakei, New Zealand in the 1950s (Brian White private communications).

Foong (2005) proposed a new TOC design that minimises water creep, reduces pressure drop, improves settling efficiency and allow a better access (than BOC) to the inside of the separator during maintenance.

However none of these designs have made it to commercial use with geothermal steam power plants and it is likely that the BOC and the horizontal separators will remain the main designs used in the foreseen future.

8. Conclusions

Steam-water separators have enabled the utilisation of liquid dominated reservoir for electricity generation and direct steam

use. High separation efficiency is sought, as it results in long life of turbine blades and low maintenance cost.

Separator pressure is chosen through optimum power output calculations while minimising and preventing silica scaling. Amorphous silica has been reported to deposit mainly at the bottom of the separator vessel.

The vertical cyclone (BOC) separators and the horizontal separators are the two popular designs adopted widely for geothermal application. Based on the reported data; 70% of power plants use vertical separators while 30% use horizontal separators.

The basic design calculations for sizing the different types of separators are summarised in this work and the advantages and the disadvantages of the different designs are also outlined.

The selection of the design is mostly based on the preference and the experience of the plant owner/operator or the technology provider.

The vertical BOC separator with spiral inlet is the most common design currently used by the industry, while the TOC and the tangential inlet separators are no longer being used.

The calculated efficiency of the BOC separator typical ranges between 99.5% and 99.99%, by maintaining an inlet velocity between 30 m/s and 40 m/s, which is lower than the breakdown velocity (42 m/s). However, data presented in this work, show that higher inlet velocities are possible in separators with smaller body diameters.

It is acknowledged that the actual separator efficiency η_s is higher than the calculated/effective efficiency η_{eff}, since some brine carryover will inevitably takes place. This can be related to changing operating conditions, mass flow rate and enthalpy (dryness) with the changes in the reservoir, the decommissioning of some wells and the introduction of new wells with time. The actual separator efficiency can only be measured indirectly after construction of the separator using chemical sampling methods and will partly be a function of fluid conditions.

The location of the separator in relation to the power station is of utmost importance. Recent experience showed that steam power plants having a centralised separator/separation station near the power house is not ideal, due to mineral and moisture damage to the turbine. It is recommended to have the separator to be located at some distance (~400 m) from the power station (Juliusson et al., 2005) to allow good scrubbing of dissolved solids and moisture removal through multiple deep drain pots.

The CFD analysis provides a visual insight to the two-phase behaviour inside the separator, a feature that cannot be achieved from any of the empirical approaches. The pressure distribution patterns and velocity profiles agree relatively well with the existing theory and therefore the results presented indicate that CFD is a promising tool which can be used to optimise separator design. However, further model refinement and validation is needed.

Acknowledgements

The authors would like to thank Mr. Yasir Al-Hilali for his help in formatting the manuscript, Mr. Brian White (NZGA) for his valuable comments and Mr. Chris Morris, Contact Energy for the valuable discussions, feedback and for providing the old separator test data. Finally, three anonymous reviewers helped to improve the manuscript.

References

Adiprana, R., Izzuddin, Yuniarto, E., 2010. Gunung Salak geothermal power plant experience of scaling/deposit: analysis, root cause and prevention. In: Proceedings of the World Geothermal Congress, Bali, Indonesia.

Albertsson, A., Porolfsson, G., Jonsson, J., 2010. Three decades of power generation – Svartsengi Power Plant. In: Proceedings of the World Geothermal Congress, Bali, Indonesia.

Allen, M.D., 1977. Geothermal Two-Phase Flow: A Study of the Annular Dispersed Flow Regime. University of Auckland.

Argueta, G.G.M., 2011. Operation and Maintenance of High Temperature Geothermal Wells, Short Course on Geothermal Drilling, Resource Development and Power Plants. United Nations University Geothermal Training Programme, Santa Tecla, El Salvador.

Bangma, P., 1960. Separation of Geothermal Bores: The Development and Performance of the 30 in. Diameter Bottom Outlet Cyclone Separator. Ministry of Works, New Zealand, Report P.W. 8/13, Wairakei, August.

Bangma, P., 1961. The development and performance of a steam-water separator for use on geothermal bores. Proc. UN Conf. New Sources Energy Rome 3 (G/13), 60–77.

Barnett, P., 2007. Cost of Geothermal Power in NZ: 2007 Update. New Zealand Geothermal Association Seminars, Auckland.

Darmawan, 1988. Wellhead Separator Design for Wells DNG-7, DNG-8 and DNG-13 in Dieng Geothermal Field in Indonesia. The University of Auckland, New Zealand.

Delliou, E., 1989. Milos demonstration project, Paper presented at the European Geothermal Update: Proceedings of the Fourth International Seminar on the Results of EC Geothermal Energy Research and Demonstration, Florence.

Di Pippo, R., 1980. Ahuachapan Geothermal Power Plant, El Salvador. In: Proceedings of the Fourth Annual Geothermal Conference and Workshop, Electric Power Research Institute, Santa Cruz, CA.

Di Pippo, R., 2008. Geothermal Power Plants Principles, Applications, Case Studies and Environmental Impact, second ed. Elsevier Ltd., United Kingdom.

Di Pippo, R., 2012. Geothermal Power Plants: Principles, Applications, Case Studies and Environmental Impact, third ed. Elsevier Ltd., United States of America.

Eliasson, E.T., 2001, June. Power generation from high-enthalpy geothermal resources. GHC Bull..

Foong, K.C., 2005. Design concept for a more efficient steam-water separator. In: Proceedings of the World Geothermal Congress, Antalya, Turkey.

Fournier, R.O., 1986. Reviews in economic geology. In: Berger, B.R., Bethke, P.M. (Eds.), Geology and Geochemistry of Epithermal Systems, vol. 2. Society of Economic Geologists, pp. 45–61.

Fournier, R.O., Rowe, J., 1977. Solubility of amorphous silica in water at high temperatures and high pressure. Am. Mineral. 62, 1052–1056.

Fuji, 2011. Consulting Service Report for Investigation of Berlin Geothermal Power Plant in Republic of El Salvador. Fuji Electric System Japan Consulting Institute.

Gerunda, A., 1981. How to size liquid–vapor separators. Chem. Eng. 88, 81–84.

Grassiani, M., 2000. Siliceous scaling aspects of geothermal power generation using binary cycle heat recovery. Trans. Geotherm. Resour. Counc., 475–478.

Gunnlaugsson, E., 2012. The Hellisheidi Geothermal Project – Financial Aspects of Geothermal Development, Short Course on Geothermal Development and Geothermal Wells. UNU-GTP and LaGeo, Santa Tecla, El Salvador.

Harrison, R.F., 1975. Methods for the Analysis of Geothermal Two-Phase Flow. University of Auckland, 204pp.

Hoffmann, A.C., Stein, L.E., 2007. Gas Cyclones and Swirl Tubes; Principles, Design and Operation, second ed. Springer, New York.

Horie, T., 2001. Berlin geothermal power plant. Fuji Electr. Rev. 47 (4), 108–112.

Horie, T., 2009. Kawerau and Nga Awa Purua Geothermal Power Station Projects, New Zealand. Fuji Electr. Rev. 55 (3), 80–86.

Juliusson, B.M., Palsson, B., Gunnarsson, A., 2005. Krafla Power Plant in Iceland – 27 years of operation. In: Proceedings of the World Geothermal Congress, Antalya, Turkey.

Jung, D.B., Wai, K.K., 2000. Boundary layer inline separator scrubber. In: Proceedings of the World Geothermal Congress, Kyushu, Tohoku, Japan, pp. 3189–3191.

Kozaki, K., 1982. Fuji geothermal power plant. Fuji Electr. Rev. 28 (4), 123–130.

Lazalde-Crabtree, H., 1984. Design approach of steam-water separators and steam dryers for geothermal applications. Geotherm. Resour. Counc. Bull., 11–20.

Lee, K.C., 1982. Performance tests of the condensate drain pots at Wairakei. In: Proceedings of the Pacific Geothermal Conference, New Zealand, pp. 123–129.

Lee, K.C., 1995. Performance of a Model In-Line Vortex Separator. World Geothermal Congress, Florence, Italy.

Legmann, H., 1999. Rotokawa geothermal combined-cycle power plant. Bull. d'Hydrogeologie 17, 425–431.

Legmann, H., Sullivan, P., 2003. The 30 MW Rotokawa I Geothermal Project five years of operation. In: International Geothermal Conference, Reykjavic.

Leith, D., Licht, W., 1972. The collection efficiency of cyclone type particle collectors: a new theoretical approach. AICHE Symp. Ser. 68 (126), 196–206.

Mandhane, J.M., Gregory, G.A., Aziz, K., 1974. A flow pattern map for gas–liquid flow in horizontal pipes. Int. J. Multiphase Flow 1, 537–553.

McKibbin, R., 1998. Fluid flow in a flashing cyclone separator. In: Proceedings of the 20th NZ Geothermal Workshop, New Zealand.

Moghaddam, A.R., 2006. A Conceptual Design of a Geothermal Combined Cycle and Comparison with a Single-Flash Power Plant for Well NWS-4, Sabalan, Iran. The United Nations University, Iceland.

Monterrosa, M., Lopez, F.E.M., 2010. Sustainability analysis of the Ahuachapan geothermal field: management and modelling. Geothermics 39, 370–381.

Moya, P., Nietzen, F., 2005. First 10 years of production at the Miravalles Geothermal Field, Costa Rica. In: Proceedings of the World Geothermal Congress, Antalya, Turkey.

Murakami, H., Kato, Y., Akutsu, N., 2000. Construction of the largest geothermal power plant for Wayang Windu Project, Indonesia. In: Proceedings of the World Geothermal Congress, Kyushu-Tohoku, Japan.

Pointon, A.R., Mills, T.D., Seil, G.J., Zhang, Q., 2009. Computational fluid dynamic techniques for validating geothermal separator sizing. GRC Trans. 33, 943–948.

Povarov, O.A., Nikolskiy, A.I., 2003. Modern Russian Geothermal Energy Technologies. International Geothermal Workshop, Russia.
Povarov, O.A., Nikolskiy, A.I., 2005. Experience of creation and operation of geothermal power plants in cold climate conditions. In: Proceedings of the World Geothermal Congress, Antalya, Turkey.
Povarov, O., Saakyan, V., Nikolskiy, A., Luzin, V., Tomarov, G., Saphoznikov, M., 2003. Experience of creation and operation of geothermal power plants at Mutnovsky geothermal field, Kamchatka, Russia. In: International Geothermal Conference, Reykjavic.
Purnanto, M.H., Zarrouk, S.J., Cater, J.E., 2012. CFD modelling of two-phase flow inside geothermal steam-water separator. In: Proceedings of the 34th NZ Geothermal Workshop, Auckland, New Zealand.
Shalaby, H.H., 2007. On the Potential of Large Eddy Simulation to Simulate Cyclone Separators. Chemnitz University of Technology, Chemnitz, Germany, 121pp.
Soeparjadi, R., Horton, G.D., Bradley, E., Wendt, P.E., 1998. A Review of the Gunung Salak Geothermal Epansion Project. In: Proceedings of the 20th NZ Geothermal Workshop, New Zealand, pp. 153–158.
Syah, Z., Kajo, J., Antro, Z., Raharjo, M.R., 2010. Project development of the Wayang Windu Unit 2 Geothermal Power Plant. In: Proceedings of the World Geothermal Congress, Bali, Indonesia.
Tassew, M., 2001. Effect of Solid Deposition on Geothermal Utilization and Methods of Control. The United Nations University.
Thain, I.A., Carey, B., 2009. Fifty years of geothermal power generation at Wairakei. Geothermics 38, 48–63.
Thorolfsson, G., 2005. Maintenance history of a geothermal plant: Svartsengi Iceland. In: Proceedings of the World Geothermal Congress, Antalya, Turkey.
Vargaftic, N.B., Volkov, B.N., Voljak, L.D., 1983. International tables of the surface tension of water. J. Phys. Chem. Ref. Data 12 (3), 817–820.
Villaseñor, L.B., Calibugan, A.A., 2011. Silica Scaling in Tiwi – Current Solutions, Paper presented at the International Workshop on Mineral Scaling, Manila, Philippines.
Watson, A., Brodie, A.J., Lory, P.J., 1996. The process design of steamfield pipeline systems for transient operation from liquid dominated reservoirs. In: Proceedings of the 18th NZ Geothermal Workshop, Auckland, New Zealand, pp. 53–58.
White, B.R., 1983. The Performance of the Bottom Outlet Cyclone Separators (Wairakei-Type). University of Auckland, New Zealand.
Zarrouk, S.J., Moon, H., 2014. Efficiency of geothermal power plants: a worldwide review. Geothermics 51, 142–153.
Zaroouk, S.J., Woodhurst, B.C., Morris, C., 2014. Silica scaling in geothermal heat exchangers and its impact on pressure drop and performance: Wairakei binary plant, New Zealand. Geothermics 51, 445–459.